Cellular Signalling 53 (2019) 80–89

Contents lists available at ScienceDirect

Cellular Signalling

journal homepage: www.elsevier.com/locate/cellsig

The effect of lentivirus-mediated SIRT1 gene knockdown in the ATDC5 cell line via inhibition of the Wnt signaling pathway

Fei Yu[1], Yusong Yuan[1], Dongdong Li, Yuhui Kou, Baoguo Jiang*, Peixun Zhang*

Department of Orthopedics and Trauma, Peking University People's Hospital, Beijing, China

ARTICLE INFO

Keywords:
SIRT1 gene
Wnt signaling pathway
ATDC5 cell line
Degenerative disease

ABSTRACT

SIRT1 is a highly conserved type III acetyltransferase gene located on chromosome 10 in mammals that belong to the Sirtuins family. In order to explore the effects of the SIRT1 gene in the ATDC5 cell line, an RNAi SIRT1 target sequence was designed and synthesized, aimed to knockdown the expression of SIRT1 in ATDC5 by a lentivirus. Gene chip, qrt-PCR, and WES analyses were used to detect the expression of SIRT1 and changes to the Wnt signaling pathway, while detecting any changes in proliferation and differentiation factors. The results showed that the expressions of the SIRT1 gene, mRNA, and protein were lower after transfection of the RNAi SIRT1sequence into ATDC5 cells. The Wnt signaling pathway, especially the classical pathway, was inhibited by the knockdown of SIRT1. The cartilaginous proliferation and differentiation of ATDC5 cells were simultaneously inhibited, and apoptosis was accelerated. In summary, knocking down SIRT1 gene increased the degeneration of ATDC5 cells via inhibiting the Wnt signaling pathway. We also found some novel factors related to the Wnt signaling pathway after SIRT1 gene knockdown (BIRC3, IL1RAP, PPP3CA, PPP2R2A, PPP2R5E, GSN, PPP2R1B, etc), which might provide new clues in disease research related to chondrocyte degeneration.

1. Introduction

Osteoarthritis (OA), also known as degenerative arthropathy, is a common orthopedic disease. Epidemiological statistics show that its incidence in people over 55 years old is 44%–70% [1] and it seriously affects health and places a heavy burden on the families of patients and society. OA is a chronic and irreversible degenerative disease based on degeneration of articular cartilage resulting from the death of chondrocytes, degradation of cartilage matrix, and the destruction of joint integrity. It is closely related to aging. Many researchers have confirmed that the expression of the Silent information regulator 1 (SIRT1) gene is significantly reduced in the articular cartilage of OA patients [2]. OA has also been shown to be closely related with the Wnt signaling pathway [3]. Nevertheless, its pathogenesis has not been fully elucidated and needs further study.

SIRT1 is a gene closely related to aging, a highly conserved type III acetyltransferase gene on chromosome 10 in mammals, which is highly expressed in the early embryo and in germ cells. SIRT1 is a key gene regulating cell proliferation [4], differentiation [5], senescence [6], and apoptosis [7] through many signaling pathways, such as the Wnt [8], PI3K/AKT [9], and NF-κB [10] signaling pathways. It also plays an important role in various diseases, including osteoarthritis [11], osteoporosis [12], and peripheral nerve repair [13].

The Wnt signaling pathway is very significant in organ development, the maintenance of internal environment homeostasis, and multisystem disease occurrence. It can regulate the process of OA [14] by influencing joint development, the proliferation and differentiation of chondrocytes, and biomechanic changes in cartilage and bone. Furthermore, the Wnt signaling pathway can be influenced by the change of TNF-α that results in changes in SIRT1 gene expression, thereby affecting the process of differentiation [15]. Moreover, decreased expression of the SIRT1 gene can positively regulate the Wnt receptor factor, FZD7 [16]. Therefore, the Wnt signaling pathway and SIRT1 are closely related. Nevertheless, we still know little about how SIRT1 affects OA through the Wnt signaling pathway.

In this study, RNAi was used to establish a ATDC5 cell model, in which the SIRT1 gene was knocked down. We then investigated the effect on the Wnt signaling pathway after SIRT1 gene knock down in vitro and its possible mechanism related to OA at the cellular level.

* Corresponding authors.
E-mail addresses: jiangbaoguo@vip.sina.com (B. Jiang), zhangpeixun@bjmu.edu.cn (P. Zhang).
[1] These authors contributed equally to this work.

https://doi.org/10.1016/j.cellsig.2018.09.016
Received 29 July 2018; Received in revised form 18 September 2018; Accepted 21 September 2018
Available online 25 September 2018

Table 1
Frame structure of lentivirus RNAi.

Number	5′	STEM	Loop	STEM	3′
GV248- Sirt1-RNAi-a	Ccgg	gaCCATTCTTCAAGTTTGCAA	CTCGAG	TTGCAAACTTGAAGAATGGTC	TTTTTg
GV248-Sirt1-RNAi-b	aattcaaaaa	gaCCATTCTTCAAGTTTGCAA	CTCGAG	TTGCAAACTTGAAGAATGGTC	

2. Materials and methods

2.1. The construction of a lentivirus containing the SIRT1 gene

2.1.1. The construction of the RNAi lentivirus vector

We designed the SIRT1 gene RNAi target sequence, 5 '- CCATTCT TCAAGTTTGCAA -3', based on the SIRT1 gene sequence. The GC content was 36.84%, and the starting site was 958. The vector was GV248 (Frame structure: hU6-MCS-Ubiquitin-EGFP-IRES-puromycin, Shanghai Genechem Co., Ltd.). We constructed the lentiviral vector GV248- Sirt1-RNAi-a and GV248- Sirt1-RNAi-b (Table 1). The single strand primers were synthesized by introducing the enzyme tangent sites *Age*I and *Eco*RI. The double stranded DNA was formed by primer annealing. T4 DNA ligase was used to connect the double enzyme tangent vector and the double stranded DNA was annealed. The competent cells were then transformed and positive bacterial colonies were identified with PCR (Table 2). Sequencing and plasmid extraction were carried out and the qualified plasmids were used in the follow-up experiment.

2.1.2. The package of RNAi lentivirus

293 T cells were treated 24 h before transfection. The cell density was adjusted to 5×10^6/15 mL, whereupon the cells were cultured in a 10 cm cell culture dish and incubated at 37 °C and 5% CO_2. The cells were transfected when the density reached 70%–80%. Serum-free medium was used 2 h before transfection. The prepared DNA solution (GV vector plasmid 20 μg, pHelper1.0 vector plasmid 15 μg, pHelper2.0 vector plasmid 10 μg) and transfection reagent (Shanghai Genechem Co., Ltd.) were added to the centrifuge tubes, and the total volume was 1 mL. The centrifuge tubes were incubated at room temperature for 15 min, then the transfection mixture was added to 293 T cells and cultured for 6 h. The culture medium containing the transfection mixture was abandoned. Next, cells were washed with 10 mL PBS, and then 20 mL serum (containing 10% FBS) was added to the cells, which were then cultured for 48–72 h. The 293 T cell supernatant was collected and centrifuged at 4 °C and 4000 *g* for 10 min. The supernatant was filtrated by a 0.45 μm filter and centrifuged at 4 °C and 25000 rpm for 2 h. The supernatant was discarded. Virus preservation solution was added for resuspension and the solution was centrifuged at 10000 rpm for 5 min. The supernatant was sub-packed, the 293 T cells were cultured in 96-well plates (4×10^4 cell/hole, 100 μL), the gradient diluent lentivirus particles were added and cultured for 24 h. Then complete medium were added. The expression of fluorescent protein was observed after 4 d and the virus titer was calculated.

2.2. Infection of the ATDC5 cell line

The ATDC5 cells were resuscitated and cultured in a 6 cm cell culture dish. The cells were subcultured when the density reached 80% in 6-well plates ($3–5 \times 10^4$ cell/mL, 2 mL). The lentivirus was used to infected the ATDC5 cells when the density reached 20%. The cells were then divided into two groups: the negative control and the RNAi lentivirus infected group. The MOI value was 50. The infection condition was Normal + polybrene. The culture medium was replaced after 16 h and cells were photographed after 72 h.

Table 2
Primer of identification.

Primers	Sequence (5′-3′)
Primer (+)	CCATGATTCCTTCATATTTGC
Primer (—)	ATGTCCTTCTGCTGATACTGGG

2.3. The detection of gene chip

Nano Drop 2000 and Agilent 2100 testing were used to identify RNA quality. The reaction of 3 'IVT was as follows: RNA amplification (First-Strand cDNA Synthesis at 42 °C for 2 h and maintenance at 4 °C; Second-Strand cDNA Synthesis at 16 °C for 1 h, at 65 °C for 10 min, and maintenance at 4 °C; IVT at 40 °C for 16 h and maintenance at 4 °C; fragmentation at 94 °C for 35 min and maintenance at 4 °C; hybridization at 98 °C for 10 min, at 45 °C for 3 min and maintenance at 45 °C), preparation of the poly-A RNA control, synthesis of one chain cDNA, synthesis of two chain cDNA, IVT reaction, purification of aRNA, and fragmentation of aRNA. The preparation of the hybrid began with the reaction fluid, which was heated. A total of 130 μL pre hybrid liquid was injected into the chip, which was placed into the pre hybrid furnace at 45 °C for 10 min. The pre hybrid liquid was abandoned and 130 μL hybrid liquid was injected into the chip, which was was placed into the pre hybrid furnace at 45 °C and 60 rpm for 16 h, The chip was washed and dyed by Gene Chip Fluidics Station 450 and the data was collected.

2.4. The detection of quantitative real-time PCR

Based on the known gene functions from previous studies of cartilage diseases associated with the Wnt signaling pathway and the results from the gene chip, 21 related differentially expressed genes were selected for RT-qPCR validation (Table 3). Glyceraldehyde-3-phosphate dehydrogenase (GAPDH) was used as an endogenous invariant control for data normalization. The gene primers were designed and synthesized by Shanghai Genechem Co., Ltd. A Trizol reagent kit (Shanghai Pu Fei) was used to extract total RNA. An M-MLV kit (Promega) was used to synthesize cDNA. According to the annealing temperature of each target gene, a two-step method was used to complete the amplification. The specificity of the amplified products was determined according to the melting curve. The data were analyzed by $2^{-\Delta\Delta Ct}$.

2.5. Western blot analysis

In some cases, western blot was performed with an automated system (http://www.proteinsimple.com.cn/wes.html) and total protein was extracted. For sample collection, the cells were washed twice with phosphate buffer saline (PBS), RIPA was added into the cells at 4 °C for 0.5-1 h, and the samples were transferred into EP tube and centrifuged at 4 °C and 12000 *g* for 5 min. The samples were submerged in boiling water for 10 min. The samples were centrifuged at 4 °C and 12000 *g* for 1 min, and maintained at −80 °C. In order to detect WES, the antibody was diluted and the reagent and diluted protein samples were added into the machine according to the set program. Proteins were separated at 375 V for 25 min. The samples was blocked out for 15 min, the first antibody was incubated for 30 min, and the second antibody was incubated for 30 min. The compass software for the WES automatic protein blot analysis system was used to analyze the results.

Table 3
Primer sequence.

Gene number	Gene name	Sequence (5′-3′)	Fragment size
NM_019812	SIRT1	Upstream: AGCTGGATGATATGACGC Downstream: CCCACAGGAGACAGAAAC	167
NM_009370	TGFBR1	Upstream: CAATGGGCTTAGTGTTCTGGG Downstream: TCCTGTTGGCTGAGTTGTGAC	289
NM_028032	PPP2R2A	Upstream: GAACAGGCCCGTGGAGACATA Downstream: CGCTTGCCACTTGCACAGACT	261
NM_011599	TLE1	Upstream: GCTGCGTGCTGTCCCTAAAGT Downstream: GCCGTGGTATTCTCAGTAGATG	230
NM_001079822	TCF7L1	Upstream: CCCGCTGACACCTCTCATC Downstream: ACAGTGGGTAATACGGTGACAG	143
NM_021457	FZD1	upstream: GAGTTCTGGACCAGTAATCCGC Downstream: ATGAGCCCGTAAACCTTGGTG	194
NM_007631	CCND1	Upstream: GCGTACCCTGACACCAATCTC Downstream: CTCCTCTTCGCACTTCTGCTC	183
NM_010849	MYC	Upstream: TTCATCTGCGATCCTGACGAC Downstream: CACTGAGGGGTCAATGCACTC	237
NM_011915	WIF1	Upstream: GGCGAGAACTTCACAAGCAGC Downstream: CAGCAGGAGCAGGCAAGGTAG	149
NM_010591	JUN	Upstream: GGATCGCTCGGCTAGAGGAAA Downstream: TGCTGCGTTAGCATGAGTTGG	154
NM_011577	TGFB1	Upstream: AGCCTGCCTCTTGAGTCCCT Downstream: CTCCCAAGGAAAGGTAGGTGAT	247
NM_011448	SOX9	Upstream: TACAGCGAGCAGCAGCAG Downstream: CGGAGGTGTCAGCGATGG	235
NM_009331	TCF7	Upstream: AGGTGGCATGCACTATCTCG Downstream: CCGCCTCTTCTTCTTTCCGT	129
NM_009524	Wnt5A	Upstream: ATGCAGTACATTGGAGAAGGTG Downstream: CGTCTCTCGGCTGCCTATTT	138
NM_008607	MMP-13	Upstream: GAGGGAGAAAATTCTGGGCTCT Downstream: CTTCCCCGTGTTCTCAAAGTGA	131
NM_008541	SMAD5	Upstream: AAGTAGATTCTGCCTGGGATT Downstream: CTGAACAAAGATGCTGCTGTC	151
NM_011782	ADAMTS5	Upstream: CCAAAGGTTACGGATGGGACT Downstream: CAGGGCTAAGTAGGCAGTGAAT	288
NM_001271627	RUNX2	Upstream: CCAAGTAGCCAGGTTCAACGA Downstream: GAGGAATGCGCCCTAAATCAC	230
NM_031163	COL2A1	Upstream: CTCCCAGAACATCACCTACCA Downstream: TGACGGTCTTGCCCCACTTAC	194
NM_021279	Wnt1	Upstream: CCTGATGTTTGCCCACCCTAC Downstream: CGACTCAGGCAAGTGGTTTCA	107
NM_007614	CTNNB1	Upstream: TTAGCTTATGGCAATCAAGAG Downstream: AGAGCAGACAGACAGCACCT	144
NM_001038663	MAPK1	Upstream: ACCTCCTGCTGAACACCACTT Downstream: TGCTTTCCTGGGAAGATAGGC	235
NM_008084	GAPDH	Upstream: TGGTGAAGGTCGGTGTGAAC Downstream: GCTCCTGGAAGATGGTGATGG	231

2.6. Statistical analysis

All data are expressed as mean ± SD. SPSS 20.0 was used for statistical analysis. Comparison between two groups was made with independent-sample *t*-tests. Comparisons between two groups were made with independent-sample t-tests and nonparametric tests. A P value < 0.05 was considered to be statistically significant.

3. Results

3.1. ATDC5 cell morphology

Seven days after adherence, cells were fusiform, triangular, or polygonal. The nuclei were round or oval, large, and located in the center of the cells. The cells were in good condition were used in the follow-up experiments (Fig. 1).

3.2. Fluorescence of ATDC5 cells after lentivirus infection

We made a 3–5 × 10^4/mL ATDC5 cell suspension, which was cultured in 6-well plates. A total of 20.00 μL 5E + 8TU/mL titer of the SIRT1 gene lentivirus and 5.00 μL 2E + 9TU/mL titer negative control virus were used to infected the ATDC5 cells when the density reached 20% with Normal and Polybrene and a MOI of 50. The culture medium was replaced after 16 h. Cells were photographed after 72 h. We found that most of the ATDC5 cells expressed fluorescence with good morphology. The cell infection rate was high, there was no bacteria or fungal growth, the medium was clear and transparent (Fig. 2).

3.3. Knockdown efficiency of the SIRT1 gene

The expression of the SIRT1 gene in ATDC5 cells from the negative control and RNAi lentivirus infected groups were detected by gene chip. The expression of the SIRT1 gene in the negative control group was 326.8746 ± 8.7103, and 61.0112 ± 10.2349 in the RNAi lentivirus infected group. SIRT1 gene expression was significantly different between the two groups ($P < 0.01$). The fold change was −5.4046216 (Fig. 4).

The ATDC5 cells were collected and total RNA was extracted. The expression of SIRT1 mRNA in ATDC5 cells from the negative control and RNAi lentivirus infected groups was detected by RT-qPCR. The expression of SIRT1 mRNA in the negative control group was 1.0143 ± 0.2092, and was 0.1353 ± 0.0196 in the RNAi lentivirus infected group. Differential expression of SIRT1 mRNA was found between the two groups ($P < 0.01$, Fig. 4).

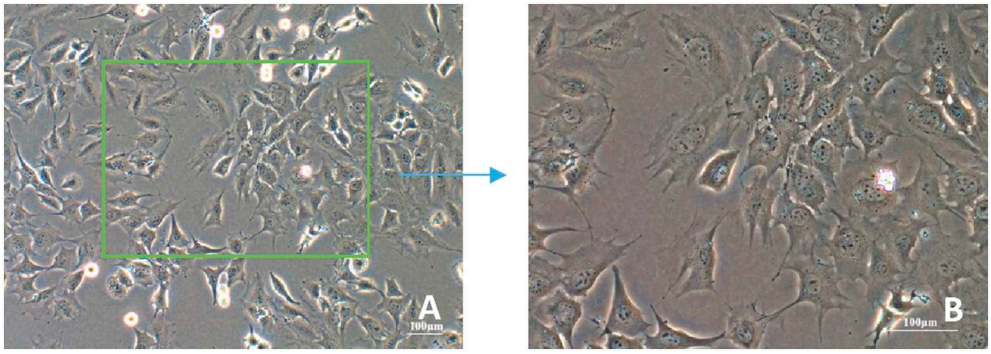

Fig. 1. The morphology of ATDC5 cells under light light microscope. A was 100×, B was 200×.

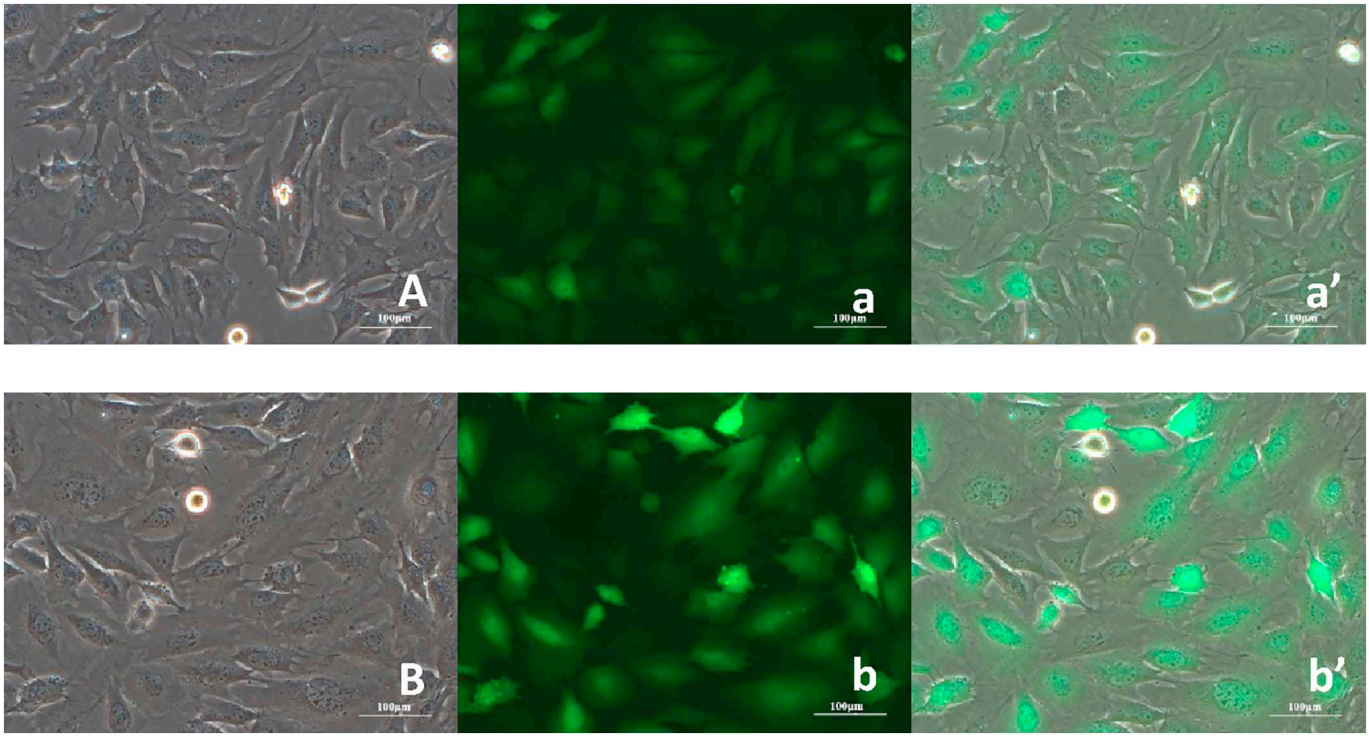

Fig. 2. The observation of ATDC5 cells after infected by the lenticirus. A, a and a' were negative control group. B, b and b' were RNAi lentivirus infected group. A and B were under bright field. a and b were fluorescence field. a' and b' were the merge of bright field and fluorescence field.

The ATDC5 cells were collected and total protein was extracted. The expression of SIRT1 (1:20) and β-actin (1:50) proteins in the negative control and RNAi lentivirus infected group cells was detected by WES. The expressions of SIRT1 and β-actin proteins in the negative control group were 103601.3333 ± 5702.8878 and 46868.0000 ± 1851.5907, respectively. The expressions of SIRT1 and β-actin proteins in the RNAi lentivirus infected group were 67.6667 ± 117.2021 and 46655.3333 ± 2269.4126, respectively (Figs. 3 & 4).

The gene chip, RT-qPCR, and WES analyses showed that the expression of the SIRT1 gene, mRNA, and protein were all decreased after lentiviral infection, confirming the successful knockout of the SIRT1 gene.

3.4. Gene changes after SIRT1 knockdown

The ATDC5 cells from the negative control and RNAi lentivirus infected groups were detected by gene chip. We detected all gene changes in mice and found that 963 genes were up-regulated and 687 were down-regulated in the RNAi lentivirus infected group compared with the negative control group (Fig. 5).

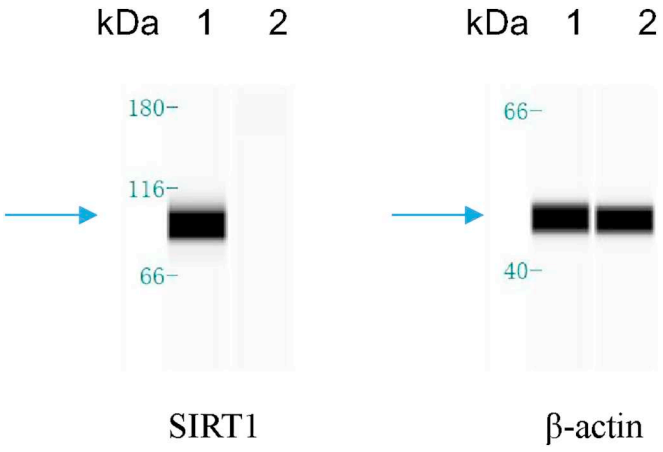

Fig. 3. Greyscale map of WES. 1 was negative control group. 2 was RNAi lentivirus infected group.

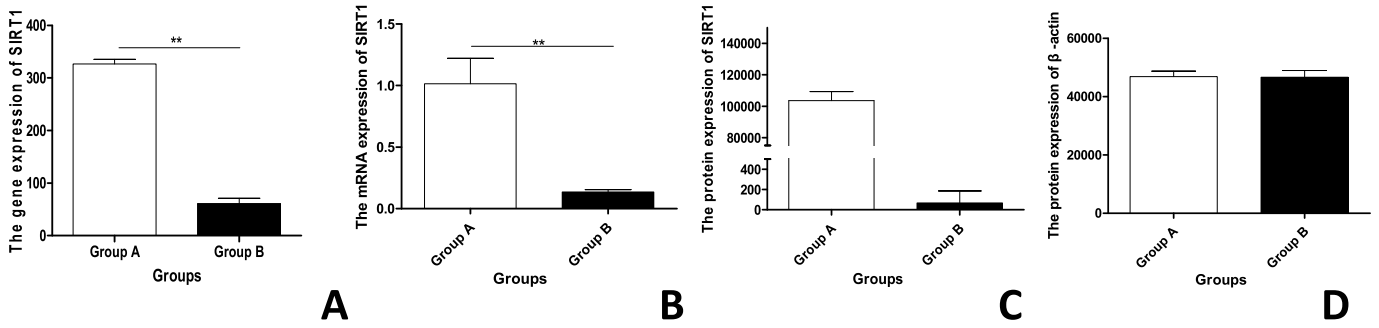

Fig. 4. The knockout of SIRT1 gene. A was the gene expression of SIRT1. B was the mRNA expression of SIRT1. C was the protein expression of SIRT1. D was the protein expression of β-actin.* was $P < 0.05$, ** was $P < 0.01$. Group A was the negative control group. Group B was the RNAi lentivirus infected group.

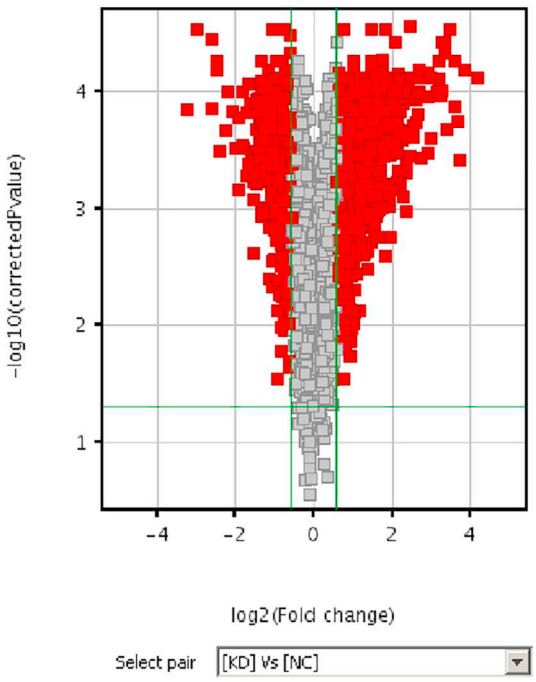

Fig. 5. Volcano map of different genes. Red indicated all probes with a difference of > 1.5 and a significant level < 0.05. (For interpretation of the references to colour in this figure legend, the reader is referred to the web version of this article.)

3.5. Detection of factors related to the Wnt signaling pathway by gene chip

The ATDC5 cells from the negative control and RNAi lentivirus infected groups were detected by gene chip. We found that the expressions of MAPK1, IL1RL1, MMP13, SMAD5, IL6, JUN, ADAMTS5, BIRC3, IL1RAP, PPP3CA, TNFRSF11B, COL1A1, PPP2R2A, SOX12, TLE1, MYC, NLK, TGFB3, TGFB2, and PPP2R5E genes were significantly increased after SIRT1 gene knock down in ATDC5 cells, while the expression of Calm1 (includes others), SP7, FZD1, ALPL, BMP1, Wnt9A, TCF7L1, GSN, XIAP, TCF7, Wnt5A, TGFBR1, PPARD, CCND1, CD44, SOX9, PPP2R1B, WIF1, RUNX2, TGFB1, and CTNNB1 were significantly decreased (Table 4). However, the expressions of the COL2A1 and Wnt1 genes were up-regulated and down-regulated, respectively, but the differences were not significant.

3.6. Detection of factors related to the Wnt signaling pathway with RT-qPCR

We chose 21 factors closely related to OA from the results of the factors detected by gene chip that were also related to the Wnt signaling pathway and detected the corresponding mRNA. ATDC5 cells were collected and total RNA was extracted. The expressions of TGFBR1, PPP2R2A, TLE1, TCFL71, FZD1, CCND1, MYC, WIF1, JUN, TGFB1, SOX9, TCF7, Wnt5a, MMP13, SMAD5, ADAMTS5, RUNX2, COL2A1, Wnt1, CTNNB1, and MAPK1 mRNAs in ATDC5 cells from the negative control and RNAi lentivirus infected groups were detected with RT-qPCR. The expressions of PPP2R2A, TLE1, MYC, JUN, MMP-13, SMAD5, ADAMTS5, COL2A1, and MAPK1 mRNAs increased in the RNAi lentivirus infected group compared with the negative control group, while the expressions of TGFBR1, TCF7L1, FZD1, CCND1, WIF1, TGFB1, SOX9, TCF7, Wnt5A, RUNX2, Wnt1, and CTNNB1 decreased (Table 5, Fig. 6).

3.7. Detection of factors related to the Wnt signaling pathway by WES

We chose four factors closely related with OA from the results of the factors detected by gene chip and RT-qPCR that were also related to the Wnt signaling pathway and detected the corresponding proteins. ATDC5 cells were collected and total protein was extracted. The expressions of CTNNB1 (1:20), MYC (1:20), JUN (1:20), Wnt5a (1:20), and β-actin (1:50) proteins in ATDC5 cells from the negative control and RNAi lentivirus infected groups were detected by WES. The expressions of the MYC and JUN proteins increased in the RNAi lentivirus infected group compared with the negative control, while the expressions of the CTNNB1 and Wnt5a proteins decreased (Table 6, Figs. 7 & 8).

4. Discussion

OA is caused by articular cartilage destruction, involving the subchondral bone and synovial fluid, typically in the small joints of the hands and weight-bearing joints. With increasing age, the incidence of OA gradually increases, and it is a common chronic degenerative disease affecting human health with a high incidence on disability [17]. There are no distinct or racial differences in disease prevalence, but OA has caused a great deal of medical and health expenditure and is a heavy burden on patients and families. At present, the pathogenesis of OA is still unclear. It can only be treated by delaying its course or improving symptoms, in order to control the disease. Therefore, the study of the pathogenesis of OA is necessitated.

The SIRT1 gene is a type III deacetylase gene, which has been increasingly studied in recent years, and belongs to the mammalian Sirtuins family. This gene is highly evolutionarily conserved and is mainly located in the nucleus. SIRT1 plays an important role in cell survival and metabolism, regulating the aging process of the organism. Its target molecules are varied and include TGF-β [18], p53 [19], and nitric oxide [20]. It has been shown to regulate signaling pathways like Wnt [8], PI3K/AKT [9], and NF- kappa B [10]. SIRT1 affects organism metabolism [21], DNA repair [22], and resistance to oxidative stress [23], and participates in the development of OA by activing these

Table 4
The gene expression of factors related to Wnt signaling pathway.

Gene	Location	Corrected P value	Change	Fold change	Type
MAPK1	Cytoplasm	0.000203844	Up	2.08269	Kinase
IL1RL1	Plasma membrane	0.000190004	Up	2.9607034	Transmembrane receptor
MMP13	Extracellular space	0.001819762	Up	1.9546458	Peptidase
SMAD5	Nucleus	0.00047754	Up	2.1726763	Transcription regulator
IL6	Extracellular space	5.58268E-05	Up	9.101095	Cytokine
JUN	Nucleus	8.27255E-05	Up	1.9107622	Transcription regulator
ADAMTS5	Extracellular space	0.000876372	Up	2.2277825	Peptidase
BIRC3	Cytoplasm	0.002517801	Up	1.5459725	Enzyme
IL1RAP	Plasma membrane	0.005012966	Up	1.5462564	Transmembrane receptor
PPP3CA	Cytoplasm	0.001475141	Up	1.6548995	Phosphatase
TNFRSF11B	Plasma membrane	0.000113462	Up	4.771306	Transmembrane receptor
COL1A1	Extracellular space	0.001438118	Up	1.7463279	Other
PPP2R2A	Cytoplasm	0.000281662	Up	2.8978753	Phosphatase
SOX12	Nucleus	0.003195848	Up	1.6155546	Transcription regulator
TLE1	Nucleus	0.000703521	Up	1.7011591	Transcription regulator
MYC	Nucleus	0.000233843	Up	1.74392	Transcription regulator
NLK	Nucleus	0.000395423	Up	2.1421013	Kinase
TGFB3	Extracellular space	0.000615302	Up	1.5868026	Growth factor
TGFB2	Extracellular space	0.000447066	Up	1.8315444	Growth factor
PPP2R5E	Cytoplasm	0.000186489	Up	1.7619604	Phosphatase
CALM1 (includes others)	Nucleus	0.00245467	Down	−1.776887	other
SP7	Nucleus	7.60161E-05	Down	−2.2061052	Transcription regulator
FZD1	Plasma membrane	0.000265509	Down	−2.0608654	G-protein coupled receptor
ALPL	Plasma membrane	0.000421552	Down	−1.9421521	Phosphatase
BMP1	Extracellular space	0.000200306	Down	−1.9554698	Peptidase
Wnt9A	Extracellular space	0.001820709	Down	−1.5123625	Other
TCF7L1	Nucleus	0.00121226	Down	−1.6666305	Transcription regulator
GSN	Extracellular space	0.001532927	Down	−1.7110924	Other
XIAP	Cytoplasm	0.00041883	Down	−1.518782	Enzyme
TCF7	Nucleus	0.000339957	Down	−1.970835	Transcription regulator
Wnt5A	Extracellular space	0.000733461	Down	−1.5796477	Cytokine
TGFBR1	Plasma membrane	0.000209643	Down	−2.0309813	Kinase
PPARD	Nucleus	0.000874403	Down	−1.6265376	ligand-dependent nuclear receptor.
CCND1	Nucleus	3.60505E-05	Down	−6.258003	Transcription regulator
CD44	Plasma membrane	0.000395423	Down	−1.7050471	Enzyme
SOX9	Nucleus	0.000957176	Down	−1.6208072	Transcription regulator
PPP2R1B	Plasma membrane	0.000406005	Down	−1.5922691	Phosphatase
WIF1	Extracellular space	0.000139282	Down	−6.174163	Other
RUNX2	Nucleus	0.000545435	Down	−2.284212	Transcription regulator
TGFB1	Extracellular space	0.000349345	Down	−1.746179	Growth factor
CTNNB1	Nucleus	0.000307204	Down	−1.5334754	Transcription regulator

Table 5
The mRNA expression of factors related to Wnt signaling pathway.

Gene	Expression 1	Expression 2	P value	Change	Fold change
PPP2R2A	1.0253 ± 0.2894	4.7077 ± 0.8860	0.002	Up	4.7077
TLE1	1.0063 ± 0.1411	1.1223 ± 0.1325	0.358	Up	1.1223
MYC	1.0020 ± 0.0767	2.7580 ± 0.3890	0.002	Up	2.7580
JUN	1.0017 ± 0.0693	2.2577 ± 0.1185	0.000	Up	2.2577
MMP13	1.0077 ± 0.1576	1.6710 ± 0.0727	0.100	Up	1.6710
SMAD5	1.0007 ± 0.0520	3.1190 ± 0.3869	0.010	Up	3.1190
ADAMTS5	1.0080 ± 0.1552	2.2827 ± 0.0826	0.100	Up	2.2827
COL2A1	1.0053 ± 0.1313	2.0523 ± 0.0745	0.000	Up	2.0523
MAPK1	1.0077 ± 0.1530	2.5573 ± 0.4299	0.100	Up	2.5573
TGFBR1	1.0100 ± 0.1682	0.8850 ± 0.1254	0.360	Down	0.8850
TCF7L1	1.0047 ± 0.1163	0.8433 ± 0.0840	0.123	Down	0.8433
FZD1	1.0017 ± 0.0757	0.8240 ± 0.0982	0.068	Down	0.8240
CCND1	1.0040 ± 0.1081	0.1677 ± 0.0199	0.000	Down	0.1677
WIF1	1.0130 ± 0.2016	0.1900 ± 0.0036	0.019	Down	0.1900
TGFB1	1.0053 ± 0.1213	0.3973 ± 0.0171	0.001	Down	0.3973
SOX9	1.0000 ± 0.0354	0.8153 ± 0.0846	0.025	Down	0.8153
TCF7	1.0013 ± 0.0699	0.6197 ± 0.0434	0.100	Down	0.6197
Wnt5a	1.0037 ± 0.1046	0.8407 ± 0.1136	0.142	Down	0.8407
RUNX2	1.0073 ± 0.1495	0.5953 ± 0.0371	0.010	Down	0.5953
Wnt1	1.0127 ± 0.1896	0.7083 ± 0.0448	0.054	Down	0.7083
CTNNB1	1.0040 ± 0.1081	0.9093 ± 0.0680	0.269	Down	0.9093

Note: Expression 1 was the expression of mRNAs in negative control group. Expression 2 was the expression of mRNAs in RNAi lentivirus infected group.

proteins [24]. It is closely related to OA. Therefore, we designed one specific RNAi sequence aimed at the mouse SIRT1 gene and constructed it into a shRNA lentivirus carrier with green fluorescent protein. After transfecting ATDC5 cells with the lentivirus, the expression of the SIRT1 gene in ATDC5 cells was detected by gene chip, RT-qPCR, and WES. The expression of the SIRT1 gene in ATDC5 cells was found to be obviously reduced at the gene, mRNA, and protein levels after transfection. We successfully established a ATDC5 cell model, in which SIRT1 gene was knocked down. We found that there were 963 genes with increased expression and 687 genes with decreased expression. We continued studying the relationship between SIRT1 gene and OA in this cell model, in order to explain its possible mechanism.

The Wnt signaling pathway plays an important role in bone and cartilage diseases. It not only regulates the formation of bone and maintains bone mass [25], but also plays an important role in the proliferation and differentiation of chondrocytes [26]. In recent years, research has shown that the excessive activation or inhibition of the Wnt signaling pathway might lead to the occurrence and development of OA [27]. Many factors in the Wnt signal pathway can participate in the course of OA under the regulation of the SIRT1 gene [28]. The Wnt signal pathway can be divided into classical and non-classical pathways. The former mainly regulates disease progress via β–catenin [29], also called CTNNB1, while the latter plays a role mainly through signal molecules such as Wnt5a [30] and Wnt10a [31]. Studies have confirmed that the expression of the SIRT1 gene decreased significantly in osteoblasts of the

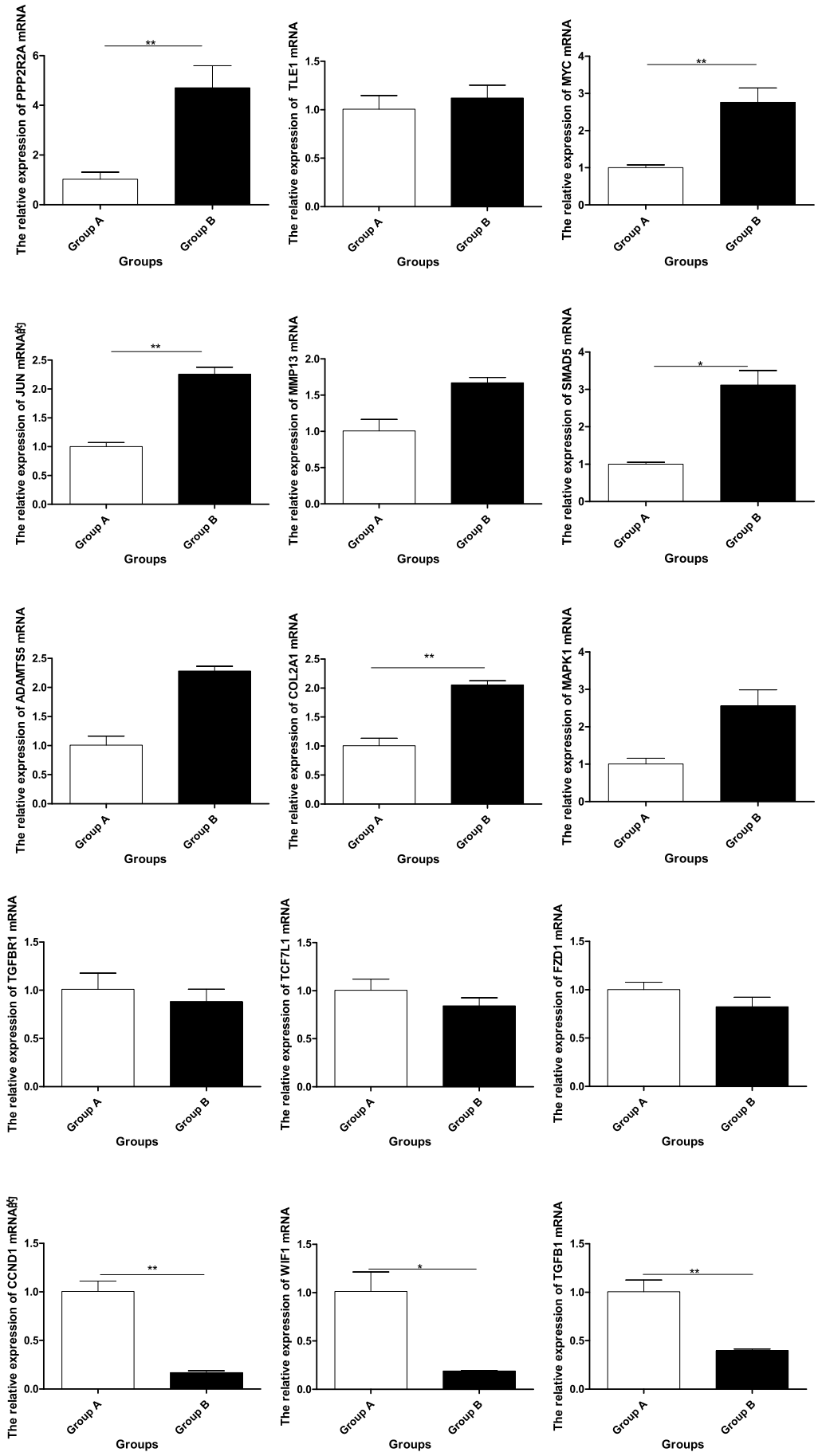

Fig. 6. The mRNA expression of factors. * was P < 0.05, ** was P < 0.01. Group A was the negative control group. Group B was the RNAi lentivirus infected group.

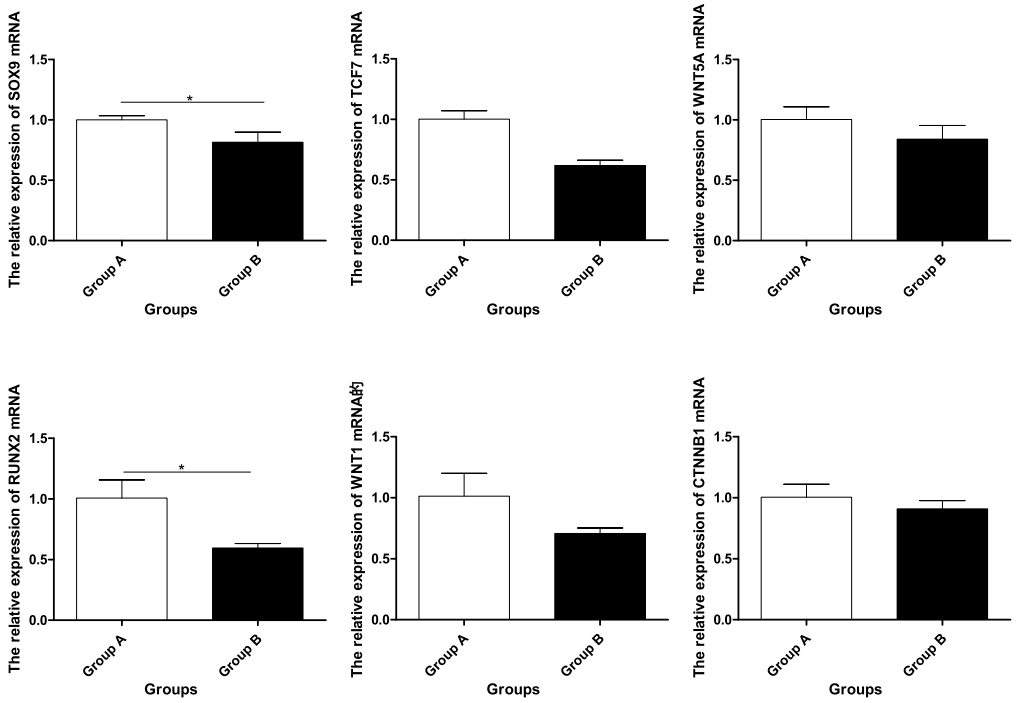

Fig. 6. (*continued*)

Table 6
The mRNA expression of factors related to Wnt signaling pathway.

Gene	Expression 1	Expression 2	P value	Change
MYC	66930.6667 ± 3662.3329	81155.6667 ± 8715.7700	0.060	Up
JUN	52138.0000 ± 5732.8120	78005.0000 ± 4797.8302	0.004	Up
CTNNB1	3713.0000 ± 97.7343	2190.3333 ± 593.9573	0.012	Down
Wnt5a	747.6667 ± 362.8778	514.6667 ± 36.5011	0.331	Down
β-actin	456668.0000 ± 8186.1903	454997.0000 ± 5277.3565	0.781	–

Note: Expression 1 was the expression of proteins in negative control group. Expression 2 was the expression of proteins in RNAi lentivirus infected group.

subchondral bone in OA patients. The down-regulation of SIRT1 has been shown to increase the expression of TGF-β 1 in osteoblasts of OA patients [28]. SIRT1 also affects differentiation from MSCs to chondrocytes through the deacetylation of β-catenin [32]. Silencing Wnt5a could also reduce the degradation of chondrocytes induced by IL-1β [33]. SIRT1 can affect the process of OA through the classical or non-classical Wnt signaling pathways. However, at present, there is little research focused on changes of chondrocytes induced by the knock-down of the SIRT1 gene and its relationship with the Wnt signaling pathway. Therefore, we focused on the influence of SIRT1 on Wnt signaling pathway after the SIRT1 gene was knocked down in ATDC5 cells.

In our research, we detected many factors at the DNA, mRNA, and protein levels, which were closely related with the Wnt signaling pathway and OA. From the changes in CTNNB1 and Wnt5A, we speculated that the decrease of SIRT1 gene expression might be mainly mediated by the classical Wnt signaling pathway, not the non-classical. In this process, down-regulation of SIRT1 inhibited the expression of CTNNB1 and its down-stream factor TCF7, which induced a decrease of the LEF/TCF complex. As a result, CCND1, the Wnt signaling target factor, was inhibited [34], thereby inhibiting the cartilaginous proliferation and promoting the apoptosis of ATDC5 cells. SOX9 and RUNX2 play important roles in the process of cartilage development [35]. The inhibition of Wnt signaling might induce the decrease of SOX9 and RUNX2 [36,37], which reduced the ability of ATDC5 cells to differentiate into chondrocytes and inhibited their proliferation. Although in our study, the variation trend of SIRT1 and TGFB1 is different from previous studies [28]. We think that this may be due to the use of different cells or interference patterns, but this does not affect our research purposes. Moreover, the decrease of TGFB1 and the increase of SMAD5 indicated that the down-regulation of SIRT1 also affected the activity of the TGF-β/Smad signaling pathway, which is an important trigger for cartilage differentiation [38,39]. ATDC5 cells differentiated into osteoblasts instead of chondrocytes [40,41]. The increase of JUN also aggravated the trend of osteoblast proliferation [42] and accelerated cell apoptosis [43]. Moreover, the increase of MAPK1 and MYC further explained the aging [44] and apoptosis [45] of ATDC5 cells. In addition, when SIRT1was knocked down, the expression of CTNNB1 was opposite that of PPP2R2A, which was similar to the results of Hein [46]. The down-regulation of PPP2R2A might promote the proliferation of cancer cells [47]. In our study, the up-regulation of PPP2R2A showed that the decrease of SIRT1 might act on PPP2R2A through the Wnt signaling pathway and inhibit the cartilaginous proliferation of ATDC5 cells. In this process, although COL2A1expression was elevated, the function of MMP-13 and ADAMTS5 were enhanced, which could destroy the chondrocyte matrix and type II collagen and cause the degeneration of ATDC5 cells. We also found that WIF1 decreased after SIRT1 was knocked down. In this condition, the inhibition of SIRT1 on the classical Wnt signaling pathway was stronger than the activation of WIF1, so that CTNNB1 decreased. However, WIF1 [48] also had an effect on ATDC5 cells, while FZD1, Wnt1, TCF7L1, TLE1, and TGFBR1 produced an opposite effect, which were reduced or increased but not significantly.

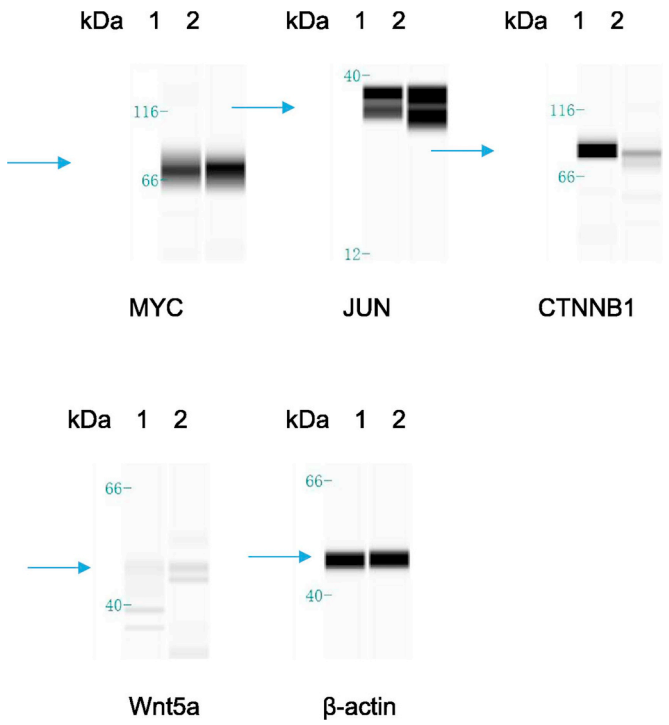

Fig. 7. Greyscale map of WES. 1 was negative control group. 2 was RNAi lentivirus infected group.

5. Conclusions

We speculate that the decrease in SIRT1 expression might inhibit the chondrogenic differentiation of ATDC5 cells via the classical Wnt signaling pathway. The knockdown of SIRT1 inhibited cartilaginous proliferation and accelerated apoptosis in ATDC5 cells, eventually inducing their degeneration. Inhibition of the classic Wnt signaling pathway might aggravate the occurrence of OA. In addition, we also found changes in factors in the Wnt signaling pathway after SIRT1 knock-down, which laid the foundation for the clinical study of OA pathogenesis and proposed new related targets.

Disclosure statement

The authors declare no conflicts of interest in this paper and are responsible alone for the content and writing.

Funding

This research was continuously funded by Chinese National Key Basic Research 973 Program [2014CB542201], Beijing science and technology new star cross subject (2018019), Beijing Natural Science Foundation [2172039], National S&T Major Project of China [SQ2018ZX100301], and Chinese National Natural Science Foundation [31571235, 31771322,51373023, 21171019, 31671248, 31640045, 31571236, 81171146,31471144, 30971526, 31100860, 31040043, 31371210, and 81372044].

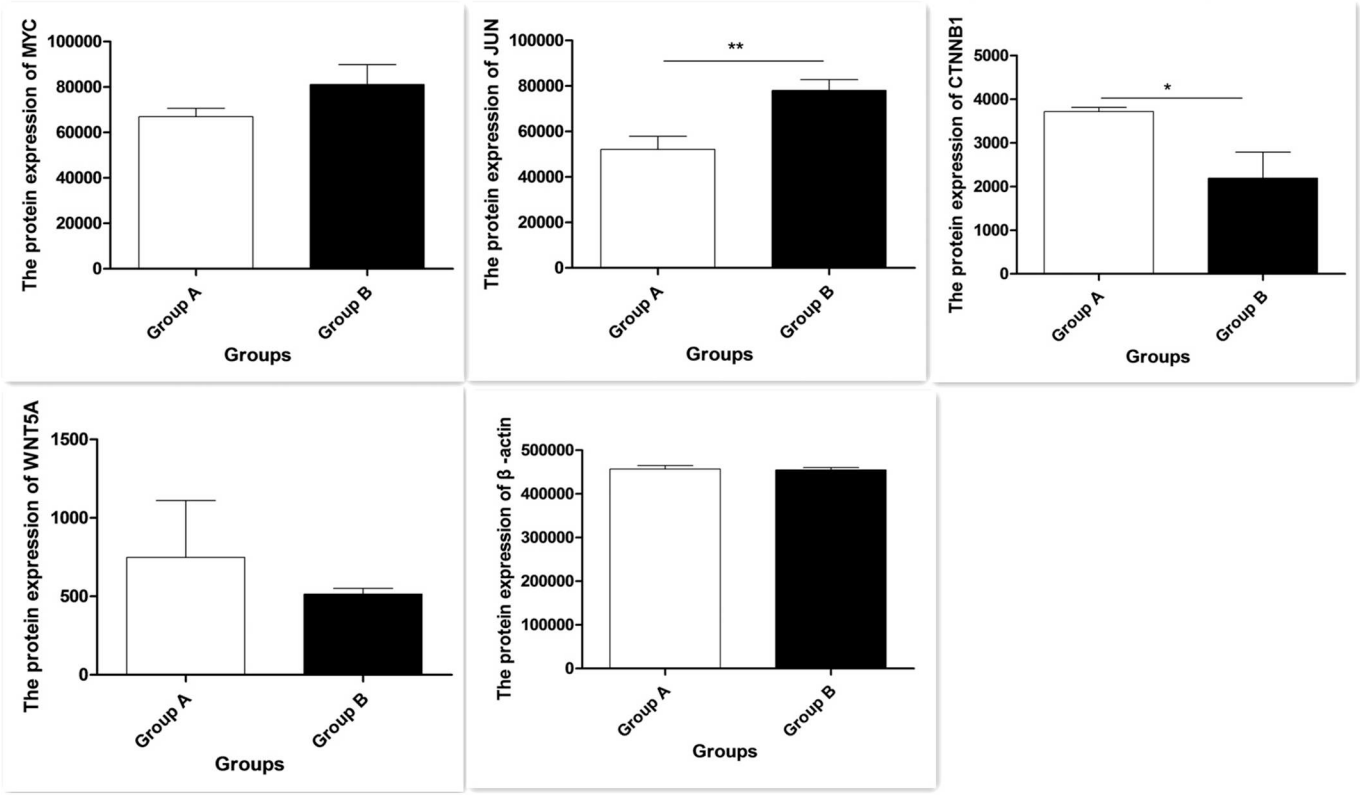

Fig. 8. The expression of each proteins. * was P < 0.05, ** was P < 0.01. Group A was the negative control group. Group B was the RNAi lentivirus infected group.

References

[1] W. Zhang, G. Nuki, R.W. Moskowitz, S. Abramson, R.D. Altman, N.K. Arden, S. Bierma-Zeinstra, K.D. Brandt, P. Croft, M. Doherty, M. Dougados, M. Hochberg, D.J. Hunter, K. Kwoh, L.S. Lohmander, P. Tugwell, OARSI recommendations for the management of hip and knee osteoarthritis:part III: changes in evidence following systematic cumulativeupdate of research published through January 2009, Osteoarthr. Cartil. 18 (2010) 476–499.

[2] Y. Li, W. Xiao, P. Wu, Z. Deng, C. Zeng, H. Li, T. Yang, G. Lei, The expression of SIRT1 in articular cartilage of patients with knee osteoarthritis and its correlation with disease severity, J. Orthop. Surg. Res. 11 (2016) 144.

[3] C. Chen, G.F. Bao, G. Xu, Y. Sun, Z.M. Cui, Altered Wnt and NF-κB Signaling in Facet Joint Osteoarthritis: Insights from RNA Deep Sequencing, Tohoku J. Exp. Med. 245 (2018) 69–77.

[4] X. Xia, X. Zhou, Knockdown of SIRT1 inhibits proliferation and promotes apoptosis of paclitaxel-resistant human cervical cancer cells, Cell. Mol. Biol (Noisy-le-grand). 64 (2018) 36–41.

[5] V.C. Khanh, A.F. Zulkifli, C. Tokunaga, T. Yamashita, Y. Hiramatsu, O. Ohneda, Aging impairs beige adipocyte differentiation of mesenchymal stem cells via the reduced expression of Sirtuin 1, Biochem. Biophys. Res. Commun. 500 (2018) 682–690.

[6] T. Liu, X. Ma, T. Ouyang, H. Chen, J. Lin, J. Liu, Y. Xiao, J. Yu, Y. Huang, SIRT1 reverses senescence via enhancing autophagy and attenuates oxidative stress-induced apoptosis through promoting p53 degradation, Int. J. Biol. Macromol. 117 (2018) 225–234.

[7] T.H. Zhang, C.M. Huang, X. Gao, J.W. Wang, L.L. Hao, Q. Ji, Gastrodin inhibits high glucose-induced human retinal endothelial cell apoptosis by regulating the SIRT1/TLR4/NF-κBp65 signaling pathway, Mol. Med. Rep. 17 (2018) 7774–7780.

[8] S. Xu, F. Sun, L. Ren, H. Yang, N. Tian, S. Peng, Resveratrol controlled the fate of porcine pancreatic stem cells through the Wnt/β-catenin signaling pathway mediated by Sirt1, PLoS ONE 12 (2017) e0187159.

[9] R. Chai, H. Fu, Z. Zheng, T. Liu, S. Ji, G. Li, Resveratrol inhibits proliferation and migration through SIRT1 mediated post-translational modification of PI3K/AKT signaling in hepatocellular carcinoma cells, Mol. Med. Rep. 16 (2017) 8037–8044.

[10] B. Niu, K. He, P. Li, J. Gong, X. Zhu, S. Ye, Z. Ou, G. Ren, SIRT1 upregulation protects against liver injury induced by a HFD through inhibiting CD36 and the NF-κB pathway in mouse kupffer cells, Mol. Med. Rep. 18 (2018) 1609–1615.

[11] F. Yu, H. Zeng, M. Lei, D.M. Xiao, W. Li, H. Yuan, J.J. Lin, Effects of SIRT1 Gene Knock-out through the Activation of SREBP2 Protein Mediated PI3K/AKT Signal Pathway on Osteoarthritis in mice, J. Huazhong. Univ. Sci. Technol. Med. Sci. 36 (2016) 683–690.

[12] X. Wang, L. Chen, W. Peng, Protective effects of resveratrol on osteoporosis via activation of the SIRT1-NF-κB signaling pathway in rats, Exp. Ther. Med. 14 (2017) 5032–5038.

[13] Y. Zhang, H. Li, Y. Cao, M. Zhang, S. Wei, Sirtuin 1 regulates lipid metabolism associated with optic nerve regeneration, Mol. Med. Rep. 12 (2015) 6962–6968.

[14] K. Miyamoto, B. Ohkawara, M. Ito, A. Masuda, A. Hirakawa, T. Sakai, H. Hiraiwa, T. Hamada, N. Ishiguro, K. Ohno, Fluoxetine ameliorates cartilage degradation in osteoarthritis by inhibiting Wnt/β-catenin signaling, PLoS ONE 12 (2017) e0184388.

[15] G. Feng, K. Zheng, D. Song, K. Xu, D. Huang, Y. Zhang, P. Cao, S. Shen, J. Zhng, X. Feng, D. Zhang, SIRT1 was involved in TNF-α-promoted osteogenic differentiation of human DPSCs through Wnt/β-catenin signal, In Vitro Cell. Dev. Biol. Anim. 52 (2016) 1001–1011.

[16] G.E. Simmons Jr., S. Pandey, A. Nedeljkovic-Kurepa, M. Saxena, A. Wang, K. Pruitt, Frizzled 7 expression is positively regulated by SIRT1 and β-catenin in breast cancer cells, PLoS ONE 9 (2014) e98861.

[17] J. Scott, C.M. Cooper, J.X. Checketts, J. Cutler, M. Boose, J. Morris, M. Vassar, An observational analysis of discontinuation and non-publication of osteoarthritis trials, Osteoarthr. Cartil. 26 (2018) 1162–1169.

[18] E.M. García-Vizcaíno, S. Liarte, J.L. Alonso-Romero, F.J. Nicolás, Sirt1 interaction with active Smad2 modulates transforming growth factor-β regulated transcription, Cell. Commun. Signal. 15 (2017) 50.

[19] Y. Wang, Z.J. Zheng, Y.J. Jia, Y.L. Yang, Y.M. Xue, Role of p53/miR-155-5p/sirt1 loop in renal tubular injury of diabetic kidney disease, J. Transl. Med. 16 (2018) 146.

[20] Z. Zhang, J. Xu, Y. Liu, T. Wang, J. Pei, L. Cheng, D. Hao, X. Zhao, H.Z. Chen, D.P. Liu, Mouse macrophage specific knockout of SIRT1 influences macrophage polarization and promotes angiotensin II-induced abdominal aortic aneurysm formation, J. Genet. Genomics. 45 (2018) 25–32.

[21] L. Rehan, K. Laszki-Szczachor, M. Sobieszczańska, D. Polak-Jonkisz, SIRT1 and NAD as regulators of ageing, Life Sci. 105 (2014) 1–6.

[22] J. Jang, Y.J. Huh, H.J. Cho, B. Lee, J. Park, D.Y. Hwang, D.W. Kim, SIRT1 Enhances the Survival of Human Embryonic Stem Cells by Promoting DNA Repair, Stem. Cell. Reports. 9 (2017) 629–641.

[23] M. Li, J. Yan, X. Chen, W. Tam, L. Zhou, T. Liu, G. Pan, J. Lin, H. Yang, M. Pei, F. He, Spontaneous up-regulation of SIRT1 during osteogenesis contributes to stem cells' resistance to oxidative stress, J. Cell. Biochem. 119 (2018) 4928–4944.

[24] L. Qiu, Y. Luo, X. Chen, Quercetin attenuates mitochondrial dysfunction and biogenesis via upregulated AMPK/SIRT1signaling pathway in OA rats, Biomed. Pharmacother. 103((2018) 1585–1591.

[25] R. Baron, F. Gori, Targeting WNT signaling in the treatment of osteoporosis, Curr. Opin. Pharmacol. 40((2018) 134–141.

[26] T. Minashima, T. Kirsch, Annexin A6 regulates catabolic events in articular chondrocytes via the modulation of NF-κB and Wnt/ß-catenin signaling, PLoS ONE 13 (2018) e0197690.

[27] R.J. Lories, M. Corr, N.E. Lane, To Wnt or not to Wnt: the bone and joint health dilemma, Nat. Rev. Rheumatol. 9 (2013) 328–339.

[28] É. Abed, D. Couchourel, A. Delalandre, N. Duval, J.P. Pelletier, J. Martel-Pelletier, D. Lajeunesse, Low sirtuin 1 levels in human osteoarthritis subchondral osteoblasts lead to abnormal sclerostin expression which decreases Wnt/β-catenin activity, Bone 59 (2014) 28–36.

[29] P. Meo Burt, L. Xiao, M.M. Hurley, FGF23 Regulates Wnt/β-Catenin Signaling-Mediated Osteoarthritis in mice Overexpressing High-Molecular-Weight FGF2, Endocrinology 159 (2018) 2386–2396.

[30] X. Martineau, É. Abed, J. Martel-Pelletier, J.P. Pelletier, D. Lajeunesse, Alteration of Wnt5a expression and of the non-canonical Wnt/PCP and Wnt/PKC-Ca2+ pathways in human osteoarthritis osteoblasts, PLoS ONE 12 (2017) e0180711.

[31] C. García-Ibarbia, J.L. Pérez-Castrillón, F. Ortiz, J. Velasco, M.T. Zarrabeitia, M. Sumillera, J.A. Riancho, Wnt-related genes and large-joint osteoarthritis: association study and replication, Rheumatol. Int. 33 (2013) 2875–2880.

[32] P. Simic, K. Zainabadi, E. Bell, D.B. Sykes, B. Saez, S. Lotinun, R. Baron, D. Scadden, E. Schipan, L. Guarente, SIRT1 regulates differentiation of mesenchymal stem cells by deacetylating β-catenin, EMBO. Mol. Med. 5 (2013) 430–440.

[33] S. Shi, Z. Man, W. Li, S. Sun, W. Zhang, Silencing of Wnt5a prevents interleukin-1β-induced collagen type II degradation in rat chondrocytes, Exp. Ther. Med. 12 (2016) 3161–3166.

[34] J. Luo, R. Yan, X. He, J. He, SOX2 inhibits cell proliferation and metastasis, promotes apoptotic by downregulating CCND1 and PARP in gastric cancer, Am. J. Transl. Res. 10 (2018) 639–647.

[35] R. Nishimura, K. Hata, Y. Takahata, T. Murakami, E. Nakamura, H. Yagi, Regulation of Cartilage Development and Diseases by Transcription Factors, J. Bone. Metab. 24 (2017) 147–153.

[36] M. Hie, N. Iitsuka, T. Otsuka, I. Tsukamoto, Insulin-dependent diabetes mellitus decreases osteoblastogenesis associated with the inhibitionof Wnt signaling through increased expression of Sost and Dkk1 and inhibition of Akt activation, Int. J. Mol. Med. 28 (2011) 455–462.

[37] A. Cheng, P.G. Genever, SOX9 determines RUNX2 transactivity by directing intracellular degradation, J. Bone Miner. Res. 25 (2010) 2680–2689.

[38] Y. Tang, J. Xiao, Y. Wang, M. Li, Z. Shi, Effect of adenovirus-mediated TGF-β1 gene transfer on the function of rabbit articular chondrocytes, J. Orthop. Sci. 22 (2017) 149–155.

[39] C.A. Hellingman, E.N. Davidson, W. Koevoet, E.L. Vitters, W.B. van den Berg, G.J. van Osch, P.M. der Kraan, Smad signaling determines chondrogenic differentiation of bone-marrow-derived mesenchymal stem cells: inhibition of Smad1/5/8P prevents terminal differentiation and calcification, Tissue. Eng. Part. A. 17 (2011) 1157–1167.

[40] M.K. Wang, H.Q. Sun, Y.C. Xiang, F. Jiang, Y.P. Su, Z.M. Zou, Different roles of TGF-β in the multi-lineage differentiation of stem cells, World. J. Stem, Cell 4 (2012) 28–34.

[41] S. Kwok, N.C. Partridge, N. Srinivasan, S.V. Nair, N. Selvamurugan, Mitogen activated protein kinase-dependent inhibition of osteocalcin gene expression by transforming growth factor-beta1, J. Cell. Biochem. 106 (2009) 161–169.

[42] N. Matsuo, S. Tanaka, M.K. Gordon, M. Koch, H. Yoshioka, F. Ramirez, CREB-AP1 protein complexes regulate transcription of the collagen XXIV gene (Col24a1) in osteoblasts, J. Biol. Chem. 281 (2006) 2452–5445.

[43] M.T. Tomicic, R. Meise, D. Aasland, N. Berte, R. Kitzinger, O.H. Krämer, B. Kaina, M. Christmann, Apoptosis induced by temozolomide and nimustine in glioblastoma cells is supported by JNK/c-Jun-mediated induction of the BH3-only protein BIM, Oncotarget 6 (2015) 33755–33768.

[44] Y. Kobayashi, S.S. Lee, R. Arai, K. Miki, M. Fujii, D. Ayusawa, ERK1/2 mediates unbalanced growth leading to senescence induced by excess thymidine in human cells, Biochem. Biophys. Res. Commun. 425 (2012) 897–901.

[45] K.E. Wiese, H.M. Haikala, B. von Eyss, E. Wolf, C. Esnault, A. Rosenwald, R. Treisman, J. Klefström, M. Eilers, Repression of SRF target genes is critical for Myc-dependent apoptosis of epithelial cells, EMBO J. 34 (2015) 1554–1571.

[46] A.L. Hein, P. Seshacharyulu, S. Rachagani, Y.M. Sheinin, M.M. Ouellette, M.P. Ponnusamy, M.C. Mumby, S.K. Batra, Y. Yan, PR55α Subunit of Protein Phosphatase 2A Supports the Tumorigenic and Metastatic potential of Pancreatic Cancer Cells by Sustaining Hyperactive Oncogenic Signaling, Cancer Res. 76 (2016) 2243–2253.

[47] H. Alder, C. Taccioli, H. Chen, Y. Jiang, K.J. Smalley, P. Fadda, H.G. Ozer, K. Huebner, J.L. Farber, C.M. Croce, L.Y. Fong, Dysregulation of miR-31 and miR-21 induced by zinc deficiency promotes esophageal cancer, Carcinogenesis 33 (2012) 1736–1744.

[48] X.S. Ge, H.J. Ma, X.H. Zheng, H.L. Ruan, X.Y. Liao, W.Q. Xue, Y.B. Chen, Y. Zhang, W.H. Jia, HOTAIR, a prognostic factor in esophageal squamous cell carcinoma, inhibits WIF-1 expression and activates Wnt pathway, Cancer Sci. 104 (2013) 1675–1682.